Received: 2 June 2020 | Revised: 20 August 2020 | Accepted: 26 August 2020

DOI: 10.1002/app.49953

ARTICLE

Applied Polymer SCIENCE WILEY

Changes in free volume and gas permeation properties of poly(vinyl alcohol) nanocomposite membranes modified using cage-structured polyhedral oligomeric silsesquioxane

Valiya Parambath Swapna[1] | **Abitha Vayyaprontavida Kaliyathan**[2] | **Vakkoottil Sivadasan Abhisha**[1] | **Hanna Joseph Maria**[2] | **Padinharu Madathil Gopalakrishnan Nambissan**[3] | **Sabu Thomas**[2] | **Ranimol Stephen**[1]

[1]Department of Chemistry, St. Joseph's College (Autonomous), Calicut, India

[2]School of Energy Materials, School of Chemical Sciences & International and Inter University Centre for Nanoscience and Nanotechnology, Mahatma Gandhi University, Kottayam, India

[3]Applied Nuclear Physics Division, Saha Institute of Nuclear Physics, Kolkata, India

Correspondence
Ranimol Stephen, Department of Chemistry, St. Joseph's College (Autonomous), Devagiri, Calicut, Kerala 673008, India.
Email: ranistephen@gmail.com

Funding information
Department of Science and Technology, Ministry of Science and Technology, India, Grant/Award Number: SR/FTP/PS-123

Abstract

The present work reports the effect of various organically functionalized polyhedral oligomeric silsesquioxane (POSS) particles on the gas transport properties (N_2, O_2, and CO_2 molecules) in poly(vinyl alcohol) (PVA) membranes. The incorporation of polyethylene glycol-POSS (PEG-POSS), octa-tetramethylammonium-POSS (Octa-TMA-POSS) and m-POSS (Octa-TMA-POSS molecule was modified using cetyltrimethyl ammonium bromide) led to the enhancement in CO_2 separation performance of PVA, among which, PEG-POSS exhibited highest CO_2 separation due to the dipole-quadrupolar interaction of CO_2 with ethylene oxide group in POSS. Octa-TMA-POSS and m-POSS reduced the O_2 and N_2 permeability of the PVA membrane due to the reduction in the number of permeating pathways as compared to pure PVA. Free volume of the membranes was evaluated by positron annihilation lifetime spectroscopic (PALS) and coincidence Doppler broadening measurements. PALS confirms the increase in polymer free volume in PVA/POSS system due to the presence of rigid and spherical POSS molecule, which could enter in the polymer chain and provide viable pathway for molecular transport. Maxwel–Wagner–Sillar and Higuchi models were applied for the theoretical prediction of permeability of the fabricated membranes.

KEYWORDS

membranes, separation techniques, thermoplastics

1 | INTRODUCTION

In recent years, polymer membrane-based gas separation processes have received remarkable attention in various fields of technology and industry like petrochemical and refinery plants all over the world. The most significant application of membrane gas separation market includes CO_2 separation from natural gas and nitrogen separation from air. In membranes, very small area is enough for the separation of gas mixtures and hence, from the economical and application points of view, polymer membranes are excellent materials for gas separation. The major advantages of polymer membranes mediated gas separation strategy over other traditional separation

processes such as adsorption, absorption, and thermal-driven cryogenic distillation, are its offered energy efficiency, low operating costs and ease of application besides the fact that it is a green approach.[1–6]

In industrial application areas such as natural gas, flue gas and bio gas processing and hydrogen purification, there is a substantial demand for energy-efficient and low cost polymer membranes for the gas mixture separation,[7–10] although the tradeoff behavior between permeability and selectivity in polymer membranes is the major disadvantage leading to a compromise on the separation performance. Therefore, recent investigations carried out by researchers focused on the fabrication of high-performing polymer membranes with efficient separation performance (simultaneously improved permeability and selectivity) and good physicochemical stability. The addition of inorganic fillers in polymer matrix is found to be a successful approach for the designing of membranes with good performance for a wide range of processes, such as transport properties. As the size of particle size decreases, the number of atoms on the particle surface increases which enhances the interfacial area in the nanocomposites. The particles might enhance or minimize the transport properties of polymers, which depends on filler characteristics, polymer-filler interaction, and method of filler incorporation in polymer matrix.[11–14]

The introduction of nanofillers to the polymer matrix often leads to a deterioration of the transport properties of the membrane, in which the nanoparticles act as barriers to minimize the passage of the gas molecules. In some cases, the addition of particulate fillers like silica and metal oxides significantly improves gas permeance and selectivity of membranes even in the case of very large penetrants. For example, there is a report by Xin et al.[12] about the fabrication of a mixed matrix membrane by incorporating differently functionalized silica in poly(ether ether ketone) (SPEEK) and pyridine functionalized silica microspheres incorporated SPEEK. The membranes exhibited remarkable gas separation performance due to the presence of large number of CO_2 interacting sites (amine group) in the membrane and enhanced polymer chain rigidification.[12] There are a number of mechanisms proposed for the improvement in gas permeation and selectivity. Particularly, the incorporation of nanoparticles in polymer, which disrupt the polymer chain packing and form polymer-particle interfacial regions or free volume pockets, will improve the permeation of gas without sacrificing selectivity. The solubility and diffusivity of gas molecules through polymer membranes depend on the available free volume within the membrane. Fine tuning of free volume in polymer matrix can be carried out by introducing bulky groups or adding fillers in the polymer.[1,16,17] The free volume pockets present in the polymer membranes can be analyzed by positron annihilation lifetime spectroscopic (PALS) techniques.[11,18–20] CO_2 gas has high solubility over light gases in polar membranes. Lin et al[21] developed various strategies to achieve high polar/nonpolar selectivity. Poly(ethylene oxide)/poly(ethylene glycol) (PEG) is well recognized for its high CO_2-philicity originated from the dipole-quadrupolar interaction between ether groups of PEG and CO_2.[22–26]

Polyhedral oligomeric silsesquioxane (POSS) nanomaterials are used to improve the gas transport performance of polymeric membranes. They are rigid silica based three-dimensional nanomaterials with the basic formula $[RSiO_{3/2}]_n$ where $n = 6–12$ and have diameters 1.5–3 nm. It is a promising nanomaterial for modifying polymer membranes and developing membranes with improved fractional free volume, thermal and mechanical properties, good gas separation performance, and long-term stability of polymer matrix.[14,27] In a recent report, it was shown that 10 wt% of PEG-POSS doped PIM-1 (most common member in polymers of intrinsic microporosity [PIMs]) membrane exhibited 150% improvement in CO_2/CH_4 selectivity with respect to pure PIM-1 and 1300 barrer permeability.[28] Poly(etherblock-amide) (PEBAX® 2533) membrane doped with 30 wt% of PEG-POSS exhibited simultaneous improvement in selectivity and permeability at 30°C.[29] In our previous work we are reported pervaporation and gas separation performance of PVA-PEO/POSS membranes.[30] It was observed that PEG-POSS greatly increased the CO_2 and water selectivity of PVA-PEO membrane. The present study focuses on the gas permeation properties of PVA membrane in the presence of three types of functionalized POSS. PEG, anionic-octa-tetramethylammonium (Octa-TMA) and cetyltrimethyl ammonium bromide (CTAB) modified POSS molecules were used to modify PVA membrane. CO_2/O_2 and CO_2/N_2 separation performance of these membranes were investigated. For a comprehensive understanding of the correlation between free volume and gas transport performance of the membrane, positron annihilation spectroscopic techniques were employed to characterize the available free volume within the membranes.[31,32]

2 | EXPERIMENTAL

2.1 | Materials and methods

Polyethylene glycol (PEG) and anionic-octa-tetramethylammonium functionalized polyhedral oligomeric silsesquioxane (PEG-POSS and Octa-TMA-POSS) were purchased from the Hybrid Plastics, Inc, (Figure 1).

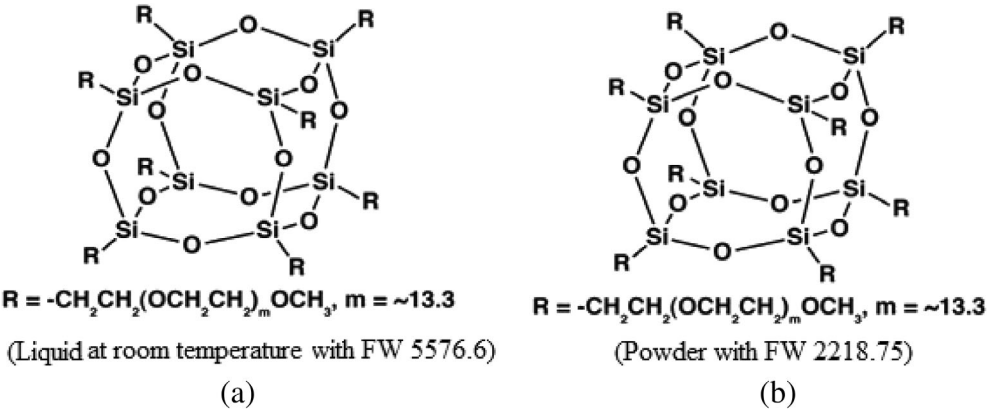

FIGURE 1 Chemical structure of (a) PEG-POSS and (b) Octa-TMA-POSS. PEG, polyethylene glycol; POSS, polyhedral oligomeric silsesquioxane; TMA, tetramethylammonium

Poly(vinyl alcohol) (PVA) (98–100 mol% hydrolyzed) of molecular weight of 125,000 g/mol was procured from the Hi-Media Laboratories Pvt. Ltd, Mumbai, India. Glutaraldehyde (GLA) (25 vol%) was obtained from the Merck India Pvt. Ltd, Mumbai, India. Cetyltrimethyl ammonium bromide (CTAB) was collected from the Sigma Aldrich.

The details of preparation of PVA-POSS membranes were presented in our previous work.[33] The samples were coded as PPP1, PPP3, POTP1, and POTP3 where PPP and POTP represents PVA/PEG-POSS and PVA/Octa-TMA-POSS, respectively, and the numbers represent the wt% of POSS. CTAB modified Octa-TMA-POSS is coded as m-POSS. The procedure for the synthesis of crosslinked PVA/m-POSS has been described in yet another of our previous works.[34] The fabricated 1 and 3 wt% m-POSS incorporated PVA membranes were coded as POCPG1 and POCPG3, respectively.

2.2 | Characterization

Cryogenically fractured samples were used for the analysis of cross-section morphology of PVA/POSS membranes and is carried out in SU6600 (Hitachi, Japan) scanning electron microscope (SEM).

PALS is the unique nondestructive technique employed to estimate free volume property of the POSS incorporated PVA membrane. In the study, positrons are injected from a radioactive source (^{22}Na) to a few-tenths of mm interior of the polymer. The details were given in one of our previous works.[30]

The LYSSY AG L 100–5000 gas permeability tester was used to analyze the gas permeability of N_2, O_2, and CO_2 into the membranes in manometric method at room temperature and 1 atm pressure according to ASTM standard D1434. Circular membranes with 9 cm diameter were used for the analysis and all the measurements were repeated three times.

3 | RESULTS AND DISCUSSION

3.1 | Morphology of PVA/POSS membranes

Morphology of the polymer membrane is the key factor that affects its gas transport performance. The field emission-scanning electron microscopy (FE-SEM) studies of different functionalized POSS incorporated PVA membranes were carried out in order to understand the morphology with varying functional group on the POSS and the images are presented in Figure 2. The cross-sectional morphology of PEG-POSS embedded PVA membrane (Figure 2(b)) shows a smooth and dense structure like pure PVA without forming any bulky agglomeration or any noticeable defects at the PVA-POSS interface.[34–37] This can be attributed to the dominating PEG side group (92 wt%) over the rigid siloxane core in PEG-POSS resulting in good interfacial bonding between polymer and POSS. However, in the case of Octa-TMA-POSS and m-POSS doped PVA membranes, spherical shape of the POSS particle were clearly visible. This phase separated morphology can be observed due to the presence of predominant inorganic siloxane core over the side group in the Octa-TMA-POSS.

AFM images PEG-POSS-, Octa-TMA-POSS-, and m-POSS-incorporated PVA membranes are presented in our previous work.[34,35] The surface roughness parameter is found to be higher in PEG-POSS and m-POSS filled PVA membranes as compared to pure PVA whereas PVA/Octa-TMA-POSS system shows reduced surface roughness. The variation in the surface roughness by changing the functional group in POSS is probably due to the difference in the nature of interaction between the matrix and the filler at the PVA-POSS interfaces, resulting in the reorganization of chains of PVA on surfaces. PVA/PEG-POSS membrane contains larger number of PEG polar functional groups on the membrane surface that can interact with the PVA chains through

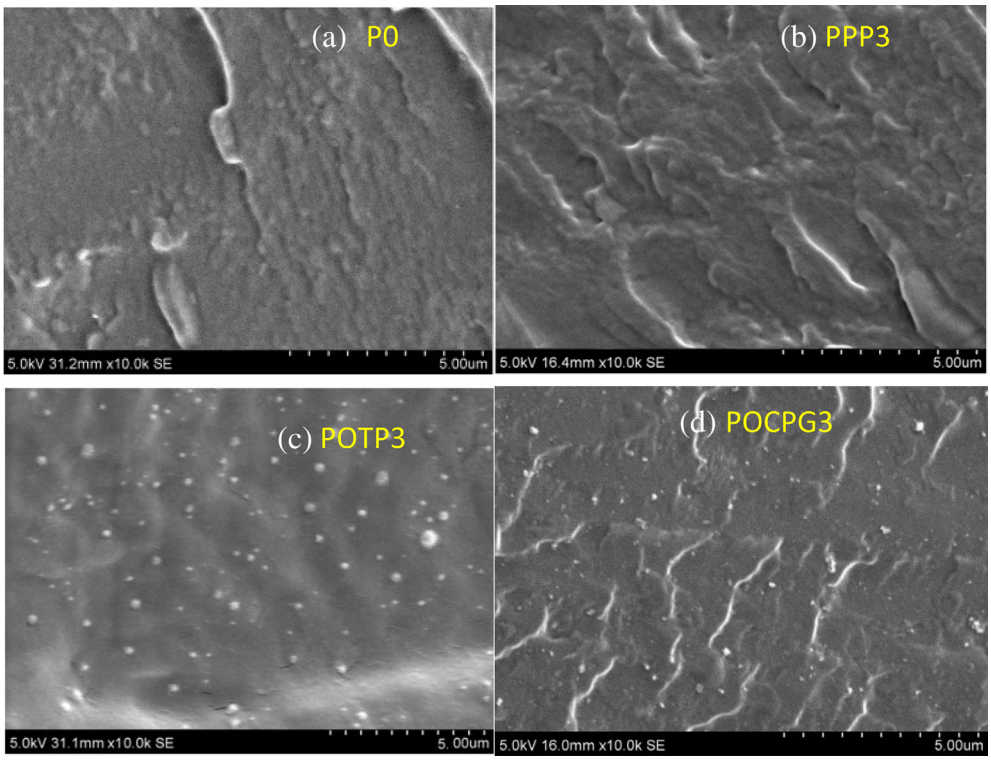

FIGURE 2 Scanning electron microscopy images of cryofractured cross section of poly(vinyl alcohol) (PVA) and different polyhedral oligomeric silsesquioxane (POSS)-embedded PVA membranes [Color figure can be viewed at wileyonlinelibrary.com]

hydrogen bonding. The Octa-TMA-POSS membrane contains less number of functional groups on the membrane surfaces to interact with PVA chains, thus resulting into reduced surface roughness as compared with pristine PVA. But, upon the modification of Octa-TMA-POSS using CTAB, the surface roughness increased due to the presence of long alkyl chains on the membrane surface, which induces new surface morphology at the PVA-m-POSS interface.

3.2 | Positron annihilation lifetime spectroscopic analysis

According to the free volume theory, the diffusion of permeant across the polymeric membrane is the outcome of random redistribution of free volume defects within the membrane. As already mentioned, PALS is a powerful and direct technique to probe free volumes within a polymer membrane. It became possible by analyzing the measured positron lifetime spectra using the PALSfit program,[38] which deconvolutes the instrumentation resolution and resolves the various positron lifetimes and their relative intensities. The peak-normalized positron lifetime spectra of the three pairs of samples along with that of pristine PVA (i.e., P0) are shown in Figure 3. Normally, three positron lifetimes and their intensities are obtained in polymeric samples, which are, respectively denoted as τ_1, τ_2, and τ_3 and I_1, I_2, and I_3. The particular lifetime and intensity of interest in the studies of polymers are τ_3 and I_3, which arise from the formation and annihilation of orthopositronium atoms (a metastable bound state of an electron and a positron with their spins aligned parallelly) within the free volume defects. A well-known model developed by Tao et al.[39] and later modified by Eldrup et al.[40] correlates the measured positronium lifetime τ_3 with the radius of the free volume cavity R by the relation.

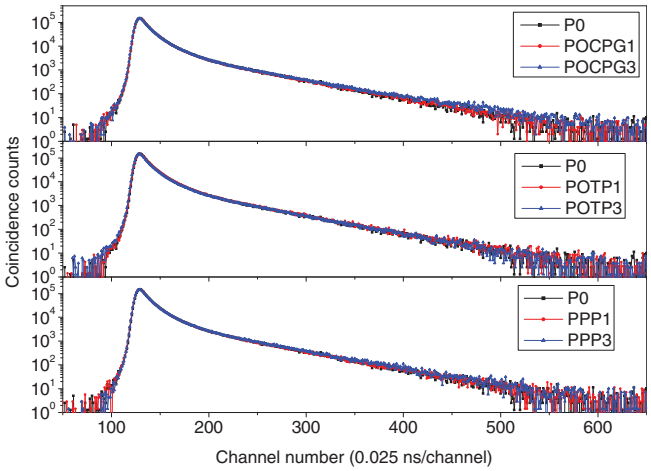

FIGURE 3 Peak-normalized positron lifetime spectra of the three pairs of samples along with pristine poly(vinyl alcohol) (i.e., P0) [Color figure can be viewed at wileyonlinelibrary.com]

TABLE 1 PALS data of PVA and PVA/POSS membranes

Sample	τ_1 (ns)	τ_2 (ns)	τ_3 (ns)	τ_4 (ns)	I_1 (%)	I_2 (%)	I_3 (%)	I_4 (%)	R_3 (Å)	R_4 (Å)	f_{v3} (%)	f_{v4} (%)
P0	0.15	Nil	1.20	2.02	78.53	Nil	18.77	2.70	1.97	2.88	1.00	0.45
PPP1	0.15	0.45	1.45	—	54.88	27.64	17.48	—	2.29	—	1.46	—
PPP3	0.17	0.50	1.54	—	59.41	23.56	17.03	—	2.41	—	1.66	—
POTP1	0.18	0.41	1.46	—	46.44	34.65	18.91	—	2.30	—	1.54	—
POTP3	0.18	0.42	1.45	—	49.89	31.12	18.99	—	2.29	—	1.53	—
POCPG1	0.12	0.45	1.48	—	58.36	24.72	16.92	—	2.32	—	1.47	—
POCPG3	0.15	0.40	1.34	2.73	49.09	31.55	17.38	1.98	2.15	3.45	1.20	0.57

Abbreviations: PALS, positron annihilation lifetime spectroscopic; POSS, polyhedral oligomeric silsesquioxane; PVA, poly(vinyl alcohol).

$$\tau_3 = 0.5\left[1 - \frac{R}{R_0} + \frac{1}{2\pi}\sin\left(\frac{2\pi R}{R_0}\right)\right]^{-1} \quad (1)$$

where $R_0 = R + \bullet R$ and $\bullet R = 1.66$ Å is an empirical parameter representing approximately the electron layer thickness of the free volume cavities. A constant A = 1/600 Å^{-3} is introduced to account for the nonsphericity of the cavities while estimating the total fractional free volume within the polymer matrix using the relation.

$$f_v = AV_f I_3, \quad (2)$$

where V_f is the volume $(4/3)\bullet R^3$ of the free volume defect.

The effect of various functionalized POSS molecules on the free volume parameters such as radius (R) of free volume hole, corresponding intensities (I_3) and fractional free volume (f_v) of PVA membrane are presented in Table 1. It can be seen from the PALS results that, in pure PVA (denoted as P0 in Table 1), both smaller (R_3) and larger sized (R_4) free volume defects are present, as indicated by an additional free volume defect component of positronium lifetime τ_4 and intensity I_4. Moreover, no τ_2 and I_2 are observed because all positrons are trapped, eventually formed positronium atoms and got annihilated from this bound state, a situation described as "saturation trapping" in positron literature.[41] Upon the incorporation of POSS molecules (i.e., in samples PPP1 and PPP3), the radius and fractional free volume of the smaller free volume cavities (R_3 and f_{v3}) are observed to have increased in the PVA membrane. The POSS molecules enter in between the polymer chains and provide a viable pathway for the transport of gas molecules owing to its rigid and spherical structure.

Large free volume cavities can be observed in the case of cetyltrimethyl ammonium functionalized POSS (m-POSS) introduced PVA membrane. It is noteworthy that in PCOPG1, all free volume defects are evenly distributed and shows only τ_3. But in PCOPG3, τ_3 and τ_4 are present, which means that the free volume defects are drifting to smaller and larger sizes. It may be noted that, unlike in the case of the reference P0 sample where $\bullet_4$ and I_4 were present at the cost of the defect-specific positron trapping component $\bullet_2$ and I_2, the positron lifetime spectrum of the PCOPG3 sample could be resolved into four distinct lifetimes and intensities, proving both the second and the fourth components arising from two separate origins, that is, the positron trapping in smaller defects and positronium formation in larger free volume defects. This can be justified on the basis of the inefficient chain packing at higher loading and the dominant nanoparticle-nanoparticle interaction over nanoparticle–polymer interaction, resulting in new voids at interfacial regions. While the intensity I_3 decreased for all POSS doped PVA, which is an indication of the decreasing number of permeating pathways in the membrane, it gets reduced in the presence of nanoparticles in the PVA matrix.

Further insight into the electron momentum specific characteristics of positrons highlighting the distribution of free volume cavities in the samples can be obtained from the analysis of the coincidence Doppler broadened spectra of the positron annihilation gamma rays acquired using energy sensitive high pure germanium detectors placed on either side of the source-sample assembly. A two-parameter spectrum of the sum and differences of the gamma ray energies E_1 and E_2 on coplanar perpendicular axes is then generated (Figure 4). The one-dimensional projection of the events within $E_1 + E_2 = 1.022 \bullet 0.00145$ MeV along the E_1 - E_2 axis is a true distribution of the longitudinal electron momenta $p_L = 2\bullet E/c$ free of background and resolution effects.[40] The projected spectra of all the samples are then divided by that of the pristine PVA sample (P0) to magnify the changes and are shown in Figure 5.

The rising curves attain maximum at around $p_L = 10.2\bullet 10^{-3}$ m_0c, which corresponds to the

momentum of the 2*p* electrons of oxygen ions or atoms. This, in turn, hints at positron trapping in free volume defects and the magnitude of the CDBS peak ratio is an indication to the concentration of such defects with respect to the reference P0 sample. Going by this argument, we find that the 1 wt% POSS-incorporated samples have more free volume holes compared to the 3 wt% POSS-incorporated ones as far as the PPP1 and PPP3 samples are concerned. This is consistent with the slightly higher value of f_{v3} that we obtained from the positron lifetime measurements (Table 1). For the case of the POTP series, the f_{v3} values did not differ significantly although the CDBS peak ratios exhibited convincing differences, which perhaps is related to the intensities I_2 of the intermediate lifetime $\bullet_2$. A noted difference is seen in the case of the 1 and 3 wt% m-POSS incorporated PVA membranes. The POCPG3 membrane has got more free volume defects when compared to POCPG1 and Table 1 has vividly displayed an additional free volume component $\bullet_4$ and I_4 in support of this observation. It may be due to the inefficient chain packing at higher loading and the dominant nanoparticle-nanoparticle interaction over nanoparticle–polymer interaction, resulting in new voids

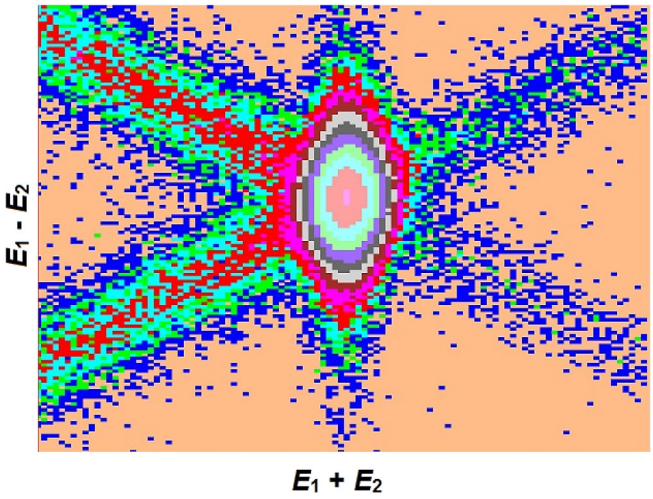

FIGURE 4 The coincidence Doppler broadened spectrum of positron annihilation gamma rays from P0 sample [Color figure can be viewed at wileyonlinelibrary.com]

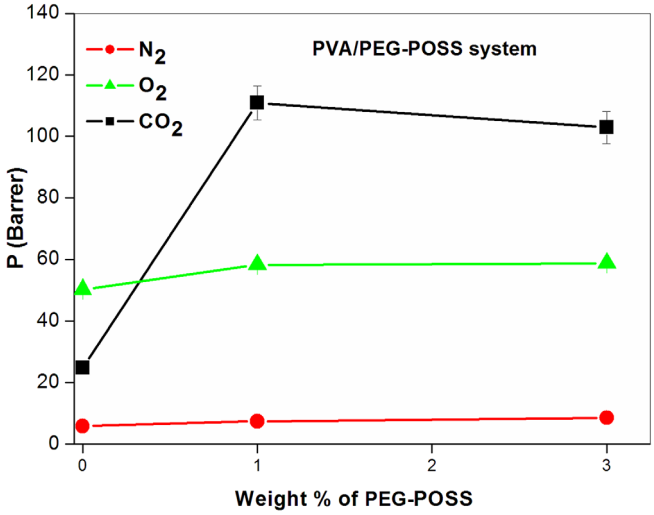

FIGURE 6 Variation in N_2, O_2, and CO_2 permeability of PVA/PEG-POSS system as a function of weight % of PEG-POSS. PEG, polyethylene glycol; POSS, polyhedral oligomeric silsesquioxane; PVA, poly(vinyl alcohol) [Color figure can be viewed at wileyonlinelibrary.com]

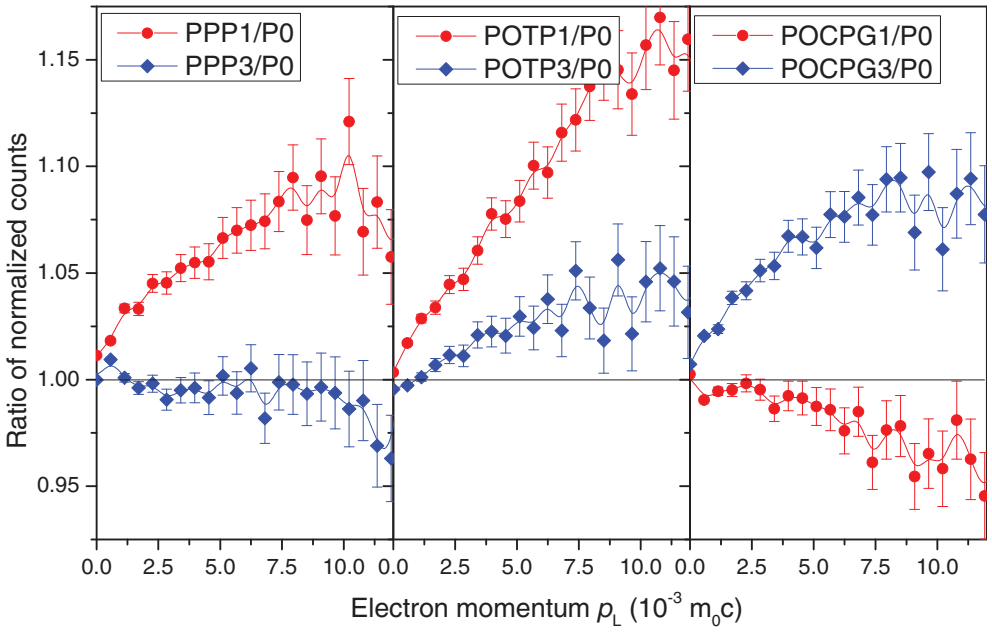

FIGURE 5 The ratio curves generated from the coincidence Doppler broadened spectra of the samples with respect to the spectrum of the pristine poly(vinyl alcohol) (P0) sample [Color figure can be viewed at wileyonlinelibrary.com]

at interfacial regions. POCPG samples are gluteraldehyde crosslinked while POTP and PPP are uncrosslinked.

3.3 | Gas separation performance of PVA/POSS membranes

The solubility and diffusivity of the penetrants in the membrane are affected by various factors such as the physical or chemical interactions between the penetrant and membrane (hydrogen bonds, polar group interactions), morphology, or chemical structure of the membrane and environmental parameters (such as pressure and temperature). The effect of different functionalized POSS molecules on the gas transport property of PVA membrane have been analyzed using nitrogen, oxygen, and carbon dioxide single gases. As seen in Figure 6, PEG-POSS doped PVA shows remarkable improvement in N_2, O_2, and CO_2 gas permeability when compared with pure PVA. PVA shows the permeability of 6, 50, and 24 barrer for N_2, O_2, and CO_2, respectively, whereas 1 wt % POSS doped PVA membrane exhibit 8, 59, and 11 barrer for N_2, O_2, and CO_2, respectively, which is due to the plasticizing action of flexible low molecular weight PEG group on POSS situated between the PVA chains. The hydrogen-bonding interaction between PVA and PEG-POSS decreases the crystallinity of the membrane and thereby construct a PVA/PEG-POSS network with high intermolecular space.[35] Consequently, the gas transport through the membranes gets improved. The improved free volume characteristics of the PVA/PEG-POSS membranes are confirmed from PALS studies too (Table 1). The high degree of roughness on the surface of the PVA/PEG-POSS membrane provides more surface area and offer large adsorption sites to the membrane than pure PVA. It is very interesting to observe that CO_2 transport across the PVA/PEG-POSS membrane is higher than O_2 and N_2 gases due to the strong dipole-quadrupolar interaction between low molecular weight polar ethyl glycol functional group on the POSS with CO_2 molecule. It is shown schematically in Scheme 1.

As shown in Figure 7 and Figure 8, PVA/Octa-TMA-POSS and PVA/m-POSS (at 1 wt%) systems exhibit reduced $N_2$and O_2 transport, which is found to be 5 and 46 for PVA/Octa-TMA-POSS and 5 and 47 for PVA/m-POSS, respectively, due to the reduction in the number of permeating pathways and improved crystallinity as compared to pure PVA.[34,35] The presence of dominant rigid crystalline siloxane core framework in Octa-TMA-POSS

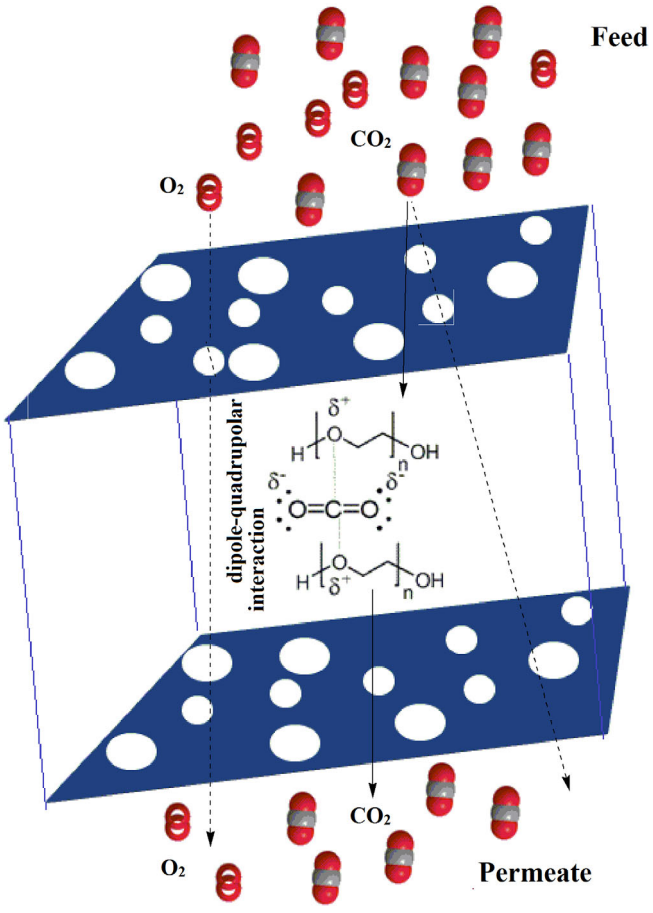

SCHEME 1 Schematic representation of the mechanism of transport of CO_2 and O_2 gas mixtures across the poly(vinyl alcohol)/polyethylene glycol-polyhedral oligomeric silsesquioxane (PEG-POSS) membranes. Dashed arrows represent the transport of gas molecules through solution-diffusion mechanism and solid arrows represent CO_2 transport due to dipole–quadrupolar interaction [Color figure can be viewed at wileyonlinelibrary.com]

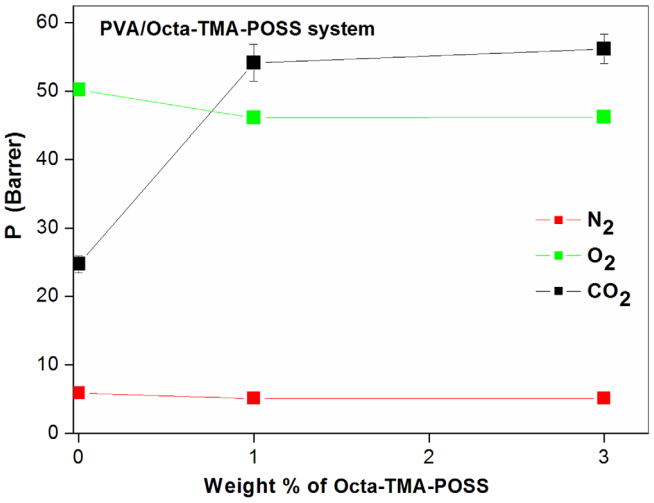

FIGURE 7 The variation in N_2, O_2, and CO_2 permeability of PVA/Octa-TMA-POSS system as a function of weight % of POSS. POSS, polyhedral oligomeric silsesquioxane; PVA, poly(vinyl alcohol); TMA, tetramethylammonium [Color figure can be viewed at wileyonlinelibrary.com]

restricts the segmental mobility of PVA chains. As a result, the permeate has to travel through more tortuous path in the membrane. A schematic representation of the diffusion path of gas molecules in pure PVA and tortuous path model in filled systems are presented in Scheme 2.

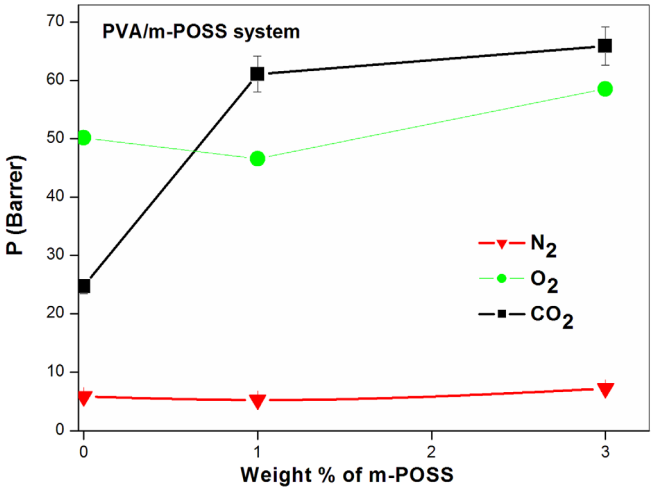

FIGURE 8 The variation in N_2, O_2, and CO_2 permeability of PVA/m-POSS membrane as a function of weight % of POSS. POSS, polyhedral oligomeric silsesquioxane; PVA, poly(vinyl alcohol) [Color figure can be viewed at wileyonlinelibrary.com]

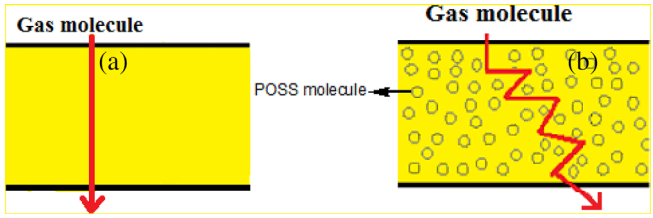

SCHEME 2 (a) Permeation path of gas molecules in pure poly(vinyl alcohol) (PVA); (b) tortuous path model in polyhedral oligomeric silsesquioxane (POSS) incorporated PVA membranes [Color figure can be viewed at wileyonlinelibrary.com]

Interestingly, the membrane shows exceptionally higher CO_2 permeance than the pure PVA, which is found to be 55 for PVA/Octa-TMA-POSS and 62 for PVA/m-POSS, respectively, owing to the high affinity of anionic POSS toward polar CO_2 molecules. Another interesting observation is the high gas permeability of 3 wt% m-POSS incorporated PVA membrane owing to the significant increase in the free volume defects in the membrane. Diffusion of gas molecules across the 3 wt% m-POSS doped PVA system is schematically presented in Scheme 3. The membrane has both larger and smaller free volume holes, consequently gas molecule can easily pass through it, which leads to high permeance and lower CO_2 selectivity.

Membranes with both high permeability and selectivity to the preferred gas are required for efficient gas separation. The permselectivity (α) of a membrane toward CO_2, O_2, and N_2 gases are computed from the expressions.

$$\alpha(CO_2, O_2) = \frac{P(CO_2)}{P(O_2)}, \quad (3)$$

TABLE 2 $CO_2/O_2(N_2)$ permselectivity values of all PVA/POSS membranes

Sample	Permselectivity $(P(CO_2)/P(N_2)$	Permselectivity $(P(CO_2)/P(O_2)$
P0	4.64	0.49
PPP1	14.82	1.97
PPP3	12.75	1.86
POTP1	10.57	1.17
POTP3	10.65	1.20
POCPG1	11.54	1.31
POCPG3	9.15	1.11

Abbreviations: POSS, polyhedral oligomeric silsesquioxane; PVA, poly(vinyl alcohol).

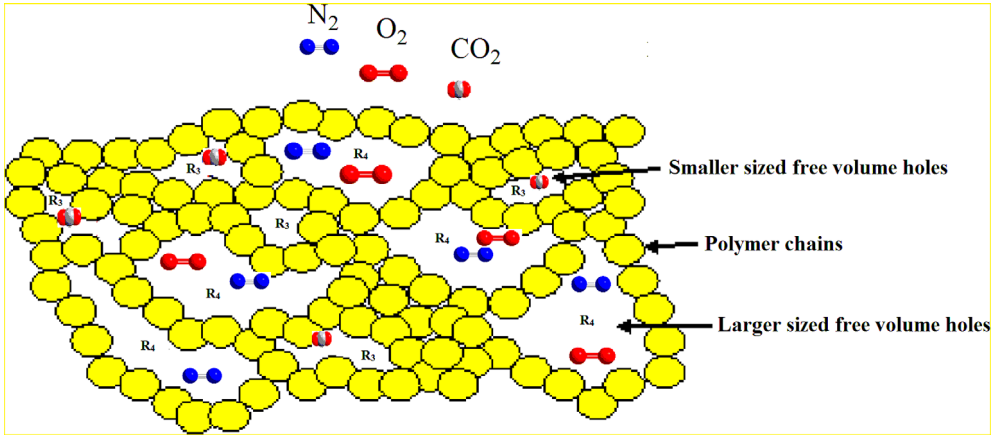

SCHEME 3 Schematic representation for the diffusion of N_2, O_2, and CO_2 molecule across the free volume of the 3 wt% m-POSS doped PVA membrane. POSS, polyhedral oligomeric silsesquioxane; PVA, poly(vinyl alcohol) [Color figure can be viewed at wileyonlinelibrary.com]

$$\alpha(CO_2, N_2) = \frac{P(CO_2)}{P(N_2)}, \quad (4)$$

where $P(CO_2)$, $P(O_2)$, and $P(N_2)$ are the permeability coefficients of CO_2, O_2, and N_2 gases, respectively.

Table 2 shows the permselectivity values of PVA/POSS membranes toward O_2, N_2, and CO_2. It is noteworthy that all membranes exhibited higher CO_2 selectivity when compared with pure PVA. It is due to the high affinity of the membrane toward CO_2 over non-polar O_2 and N_2 gases.

3.4 | Theoretical predictions of gas permeation

The gas permeability through membranes is further explored by applying modified Higuchi and Maxwel–Wagner–Sillar models.[42–45] The modified Higuchi model is given by[42]:

$$P = P_C\left(1 - \frac{6\varphi_f}{4 + 2\varphi_f - K_H\left(1-\varphi_f\right)}\right) \quad (5)$$

TABLE 3 The best fitted K_H parameters obtained for different gases in PVA/POSS membranes according to the Higuchi model

Gas	PVA/PEG-POSS	PVA/Octa-TMA-POSS	PVA/m-POSS
N_2	4.5	3.2	3.1
O_2	4.6	3.21	3.5
CO_2	4.64	4.49	4.09

Abbreviations: PEG, polyethylene glycol; POSS, polyhedral oligomeric silsesquioxane; PVA, poly(vinyl alcohol); TMA, tetramethylammonium.

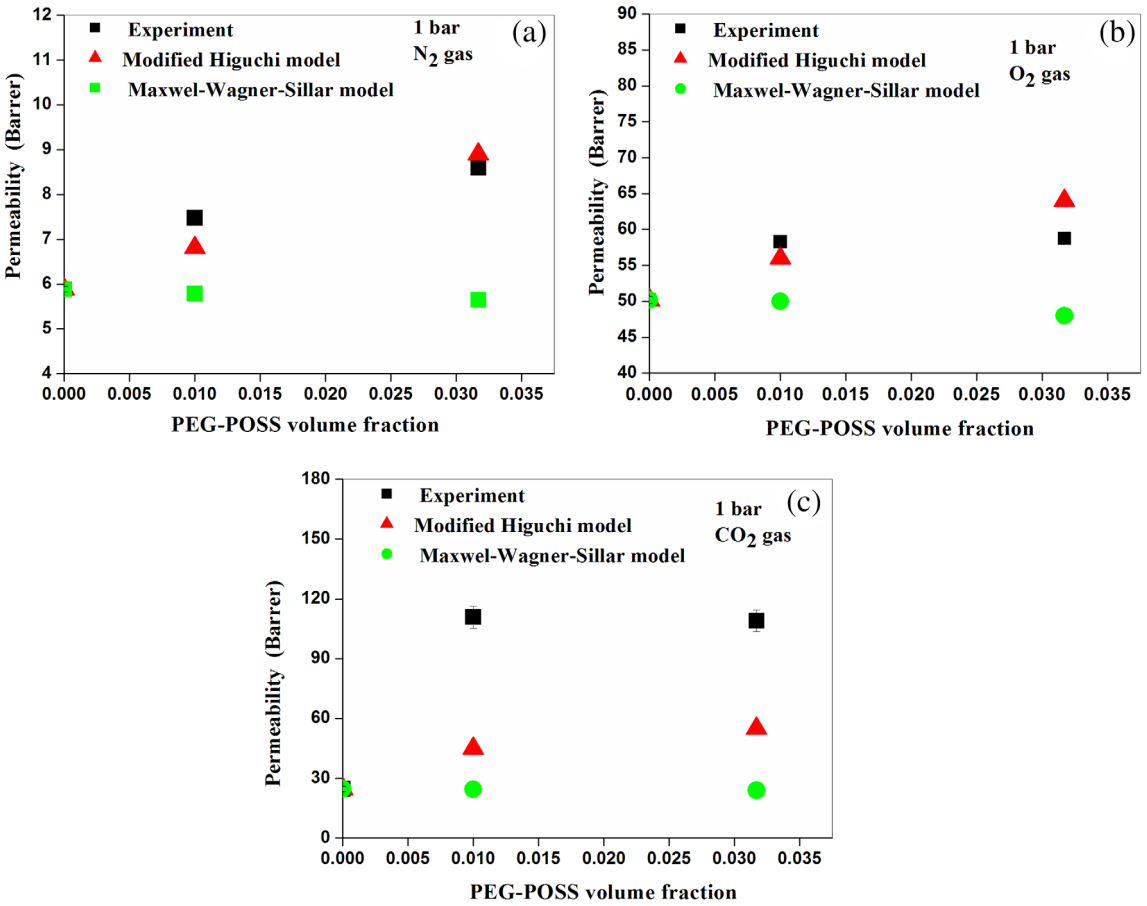

FIGURE 9 Comparison of experimental and theoretical permeability of PVA/PEG-POSS membranes for (a) N_2, (b) O_2, and (c) CO_2 gases. PEG, polyethylene glycol; POSS, polyhedral oligomeric silsesquioxane; PVA, poly(vinyl alcohol) [Color figure can be viewed at wileyonlinelibrary.com]

where P_c is the permeability of continuous PVA phase, P is the permeability of PVA/POSS system, φ_f is the volume fraction of POSS and K_H is the Higuchi constant.

Higuchi selected K_H values as 0.78 for spherical particles on the basis of experimental data.[42] According to his observations, the K_H value varies with the change in particle size. In the present work, no good agreement in gas permeability between experimental data and Higuchi model could be found when $K_H = 0.78$ because of the nanosize effect of POSS particles. Therefore, for the best fit of Higuchi model with experimental data, appropriate values of K_H are identified through least square method and are presented in Table 3. Figures 9, 10, and 11 depict the correlation between the experimental results and the Higuchi model based fit using the selected K_H parameter. It can be seen that K_H increases with increase in gas permeability through the PVA/POSS membrane. Similar observations have been reported for C-MOF-5 incorporated polyetherimide (PEI) mixed matrix membranes.[46] The order of decreasing permeability (P) and K_H are $P(CO_2) > P(O_2) > P(N_2)$ and $K_H\ (CO_2) > K_H\ (O_2) > K_H\ (N_2)$, respectively.

The other model, known as Maxwel–Wagner–Sillar model,[42,43,47] is given by the expression.

$$P = P_C \frac{nP_F + (1-n)P_C - (1-n)\varphi_f(P_C - P_F)}{nP_F + (1-n)P_C + n\varphi_f(P_C - P_F)} \quad (6)$$

In the case of nonporous impermeable spherical particle ($n = 1/3$ and $P_F = 0$) dispersed polymer membranes, the Maxwel–Wagner–Sillar model becomes:

$$P = P_C \frac{\left(\left(1-\varphi_f\right)\right.}{\left(1+0.5\varphi_f\right)} \quad (7)$$

As seen in Figures 11(a,b), N_2 and O_2 permeability of PEG-POSS dispersed PVA systems calculated from Higuchi model exhibited good agreement with the experimental data. However, the experimental CO_2 permeability is found to be higher than that predicted by the Higuchi model due to the high dipole-quadrupolar interaction of

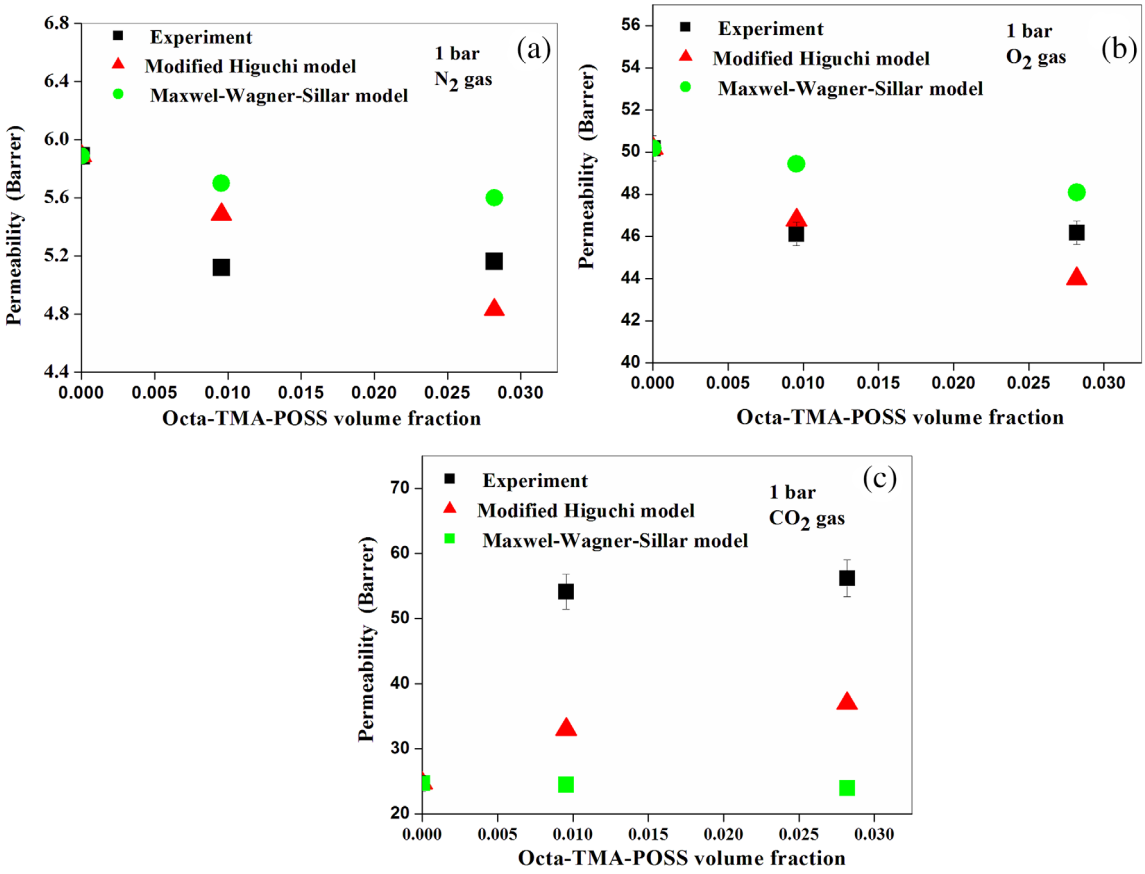

FIGURE 10 Comparison of experimental and theoretical permeability of PVA/Octa-TMA-POSS membranes for (a) N_2, (b) O_2, and (c) CO_2 gases. POSS, polyhedral oligomeric silsesquioxane; PVA, poly(vinyl alcohol); TMA, tetramethylammonium [Color figure can be viewed at wileyonlinelibrary.com]

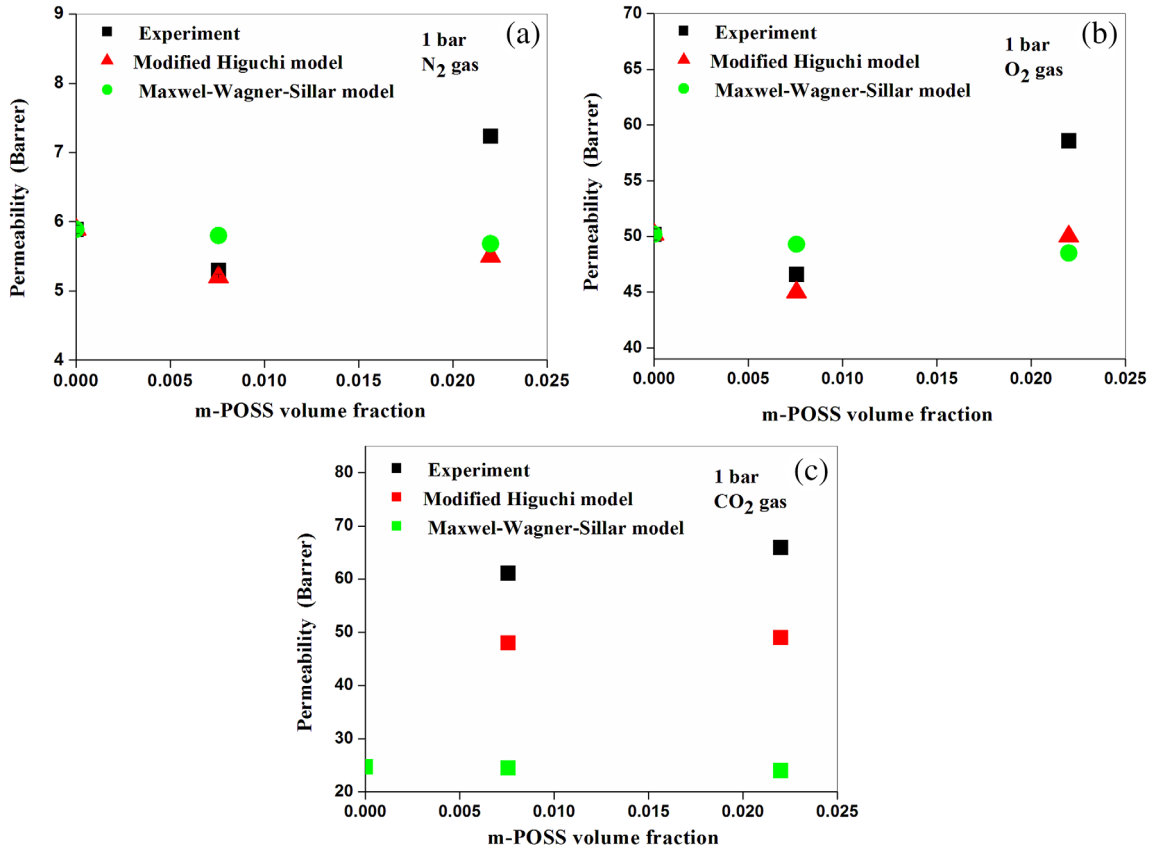

FIGURE 11 Comparison of experimental and theoretical permeability of PVA/m-POSS membranes for (a) N_2, (b) O_2, and (c) CO_2 gases. POSS, polyhedral oligomeric silsesquioxane; PVA, poly(vinyl alcohol) [Color figure can be viewed at wileyonlinelibrary.com]

CO_2 molecules with polar ethylene oxide groups (Figure 9 (c)). Similar results are observed in the case of Octa-TMA-POSS and m-POSS dispersed PVA systems (Figure 10 and Figure 11). However, for the 3 wt% of m-POSS loaded PVA system, experimental results show high permeability to all gases than the theoretical values and the reason behind this observation is the significant change in the PVA-POSS interfaces and the presence of both smaller and larger free volume holes as seen from PALS results. The Maxwel–Wagner–Sillar model is not in agreement with the experimental results because of the fact that the model is only considering the effect of volume fraction of POSS particle on the matrix. The interaction of gas molecules with the membrane and the influence of size and shape of POSS particles are not included in this model.

4 | CONCLUSIONS

In summary, the effect of different functionalized POSS particles on the permeability of N_2, O_2, and CO_2 molecules in PVA membrane were examined. The diffusion of gas molecules through the membrane was correlated to the free volume of the system, which could be evaluated by positron lifetime and coincidence Doppler broadening measurements. Free volume as well as gas diffusion observed in PVA/POSS system was higher as compared to pristine PVA. PVA/PEG-POSS membranes showed remarkable improvement in CO_2 permeability and selectivity because of the plasticizing action of flexible low molecular weight PEG group on the POSS situated between PVA chains and high dipole-quadrupolar interaction of CO_2 molecules with ethylene oxide groups present in the membrane. The introduction of Octa-TMA-POSS reduced the O_2 and N_2 permeability of the PVA membrane due to the improved crystallinity of PVA/Octa-TMA-POSS system as compared to pure PVA. The Higuchi model of permeability provided good agreement for the experimental data in the case of N_2 and O_2, whereas the experimental values were found to be significantly higher than the theoretical values for the permeability of CO_2 molecules due to dipole-quadrupolar interaction of CO_2 molecules with polar ethylene oxide groups. The study thus establishes a novel method of understanding the permeability properties of organic molecules incorporated polymer membranes based on their free volume defect properties and the ability to quantitatively correlate them with the help of unique experimental probes such as positron annihilation spectroscopy and gas permeability measurements.[48–51]

ACKNOWLEDGMENT

The corresponding author Ranimol Stephen is thankful to DST-SERB, New Delhi for the financial assistance through Project No. SR/FTP/PS-123/2012.

ORCID

Ranimol Stephen https://orcid.org/0000-0002-8087-6250

REFERENCES

[1] S. Hasebe, S. Aoyama, M. Tanaka, H. Kawakami, *J. Membrane Sci.* **2017**, *536*, 148.
[2] E. G. Estahbanati, M. Omidkhah, A. E. Amooghin, *Appl. Mater. Interfaces* **2017**, *9*, 10094.
[3] Y. Cheng, Z. Wang, D. Zhao, *Ind. Eng. Chem. Res.* **2018**, *57*, 4139.
[4] V.S. Abhisha, V.P. Swapna, R. Stephen, Transport Properties of Polymeric Membranes Elsevier, Amsterdam, Netherlands 2017, eBook ISBN:9780128098851.
[5] A. R. Esmaeili, N. Mir, R. Mohammadi, *J. Colloid Interface Sci.* **2020**, *573*, 317.
[6] M. Jamali, A. Moghadam, H. V. Tafreshi, B. Pourdeyhimi, *Appl. Surf. Sci.* **2018**, *456*, 626.
[7] M. Fang, Z. He, B. Timothy, C. Merkel, Y. Okamoto, *J. Mater. Chem. A* **2018**, *6*, 652.
[8] D. Wu, C. Sun, P. K. Dutta, W. S. W. Ho, *J. Membrane Sci.* **2017**, *534*, 33.
[9] L. Ansaloni, R. Rennemo, H. K. Knuutila, L. Deng, *J. Membrane Sci.* **2017**, *537*, 272.
[10] A. Ito, T. Yasuda, T. Yoshioka, A. Yoshida, X. Li, K. Hashimoto, K. Nagai, M. Shibayama, M. Watanabe, *Macromolecules* **2018**, *51*, 7112.
[11] S. Khoonsap, S. Rugmai, W. S. Hung, K. R. Lee, S. Klinsrisuk, S. Amnuaypanich, *J. Membrane Sci.* **2017**, *544*, 287.
[12] Q. Xin, Y. Zhang, Y. Shi, H. Ye, L. Lin, X. Ding, Y. Zhang, H. Wu, Z. Jiang, *J. Membrane Sci.* **2016**, *514*, 73.
[13] D. Peng, S. Wang, Z. Tian, X. Wu, Y. Wu, H. Wu, Q. Xin, J. Chen, X. Cao, Z. Jiang, *J. Membrane Sci.* **2017**, *522*, 351.
[14] V.P. Swapna, V.S. Abhisha, R. Stephen, Polymer Nanocomposite Membranes for Pervaporation, Elsevier, Amsterdam, Netherlands, 2020, eBook ISBN: 9780128167854.
[15] F. Huang, C. J. Cornelius, *J. Membrane Sci.* **2017**, *542*, 110.
[16] A. P. Isfahani, M. Sadeghi, K. Wakimoto, B. B. Shrestha, R. Bagheri, E. Sivaniah, B. Ghalei, *Appl. Mater. Interfaces* **2018**, *10*, 17366.
[17] E. Chehrazi, A. Sharif, M. Omidkhah, M. Karimi, *Appl. Mater. Interfaces* **2017**, *9*, 37321.
[18] Z. X. Low, P. M. Budd, N. B. McKeown, D. A. Patterson, *Chem. Rev.* **2018**, *118*, 5871.
[19] S. K. Sharma, P. K. Pujari, *Prog. Polym. Sci.* **2017**, *75*, 31.
[20] C. R. Bilchak, *Macromolecules* **2017**, *50*, 7111.
[21] H. Lin, B. D. Freeman, *J. Mol. Stru.* **2005**, *739*, 57.
[22] A. P. Isfahani, M. Sadeghi, K. Wakimoto, A. H. Gibbons, R. Bagheri, E. Sivaniah, B. Ghalei, *J. Membrane Sci.* **2017**, *542*, 143.
[23] L. Khounlavong, V. Pryamitsyn, V. Ganesan, *J. Chem. Phys.* **2010**, *133*, 144904.
[24] J. M. Kropka, V. Pryamitsyn, V. Ganesan, *Phys. Rev. Lett.* **2008**, *101*, 075702.
[25] M. Galizia, M. G. D. Angelis, M. Messori, G. C. Sarti, *Ind. Eng. Chem. Res.* **2014**, *53*, 9243.
[26] M. Md, V. Rahman, S. Filiz, C. Shishatskiy, P. Abetz, M. M. Georgopanos, S. Khan, V. A. Neumann, *Appl. Mater. Interfaces* **2015**, *7*, 12289.
[27] Y. Kinoshita, *J. Membrane Sci.* **2017**, *539*, 178.
[28] L. Yang, Z. Tian, X. Zhang, X. Wu, Y. Wu, Y. Wang, D. Peng, S. Wang, H. Wu, Z. Jiang, *J. Membrane Sci.* **2017**, *543*, 69.
[29] M. M. Rahman, *J. Membrane Sci.* **2013**, *437*, 286.
[30] V. P. Swapna, P. M. G. Nambissan, S. P. Thomas, V. K. Abitha, T. Jose, S. C. George, S. Thomas, R. Stephen, *Poly. Int.* **2019**, *68*, 1280.
[31] Y. C. Jean, J. P. Yuan, J. Liu, Q. Deng, H. Yang, *J. Poly. Sci. Part B: Poly. Phys.* **1995**, *33*, 2365.
[32] C. Nagel, K. Günther-Schade, D. Fritsch, T. Strunskus, F. Faupel, *Macromolecules* **2002**, *35*, 2071.
[33] V. P. Swapna, D. Ponnamma, K. K. Sadasivuni, S. Thomas, R. Stephen, *J. Appl. Polym. Sci.* **2017**, *134*, 45447.
[34] V. P. Swapna, T. Jose, G. Moni, S. C. George, P. S. Thomas, S. Thomas, R. Stephen, *J. Mater. Sci.* **2019**, *54*, 8319.
[35] V. P. Swapna, T. Jose, S. C. George, S. Thomas, R. Stephen, *J. Appl. Polym. Sci.* **2019**, *136*, 47060.
[36] C. H. Jung, I. T. Hwang, C. H. Jung, J. H. Choi, *Radiat. Phy. Chem.* **2014**, *102*, 23.
[37] H. Pan, Z. Qiu, *Macromolecules* **2010**, *43*, 1499.
[38] J. V. Olsen, P. Kirkegaard, N. J. Pedersen, M. Eldrup, *Phys. Status Solidi C* **2007**, *4*, 4004.
[39] S. J. Tao, *J. Chem. Phy.* **1972**, *56*, 5499.
[40] M. Eldrup, D. Lightbody, J. N. Sherwood, *Chem. Phys.* **1981**, *63*, 51.
[41] R. N. West, *Adv. Phys.* **1973**, *22*, 263.
[42] W. I. Higuchi, *J. Phy. Chem.* **1958**, *62*, 649.
[43] M. Sadeghia, M. A. Semsarzadehb, M. Barikanic, M. P. Chenar, *J. Membrane Sci.* **2011**, *376*, 188.
[44] H. V. Thang, S. Kaliaguine, *Chem. Rev.* **2013**, *113*, 4980.
[45] A. Idris, Z. Man, A. S. Maulud, F. Uddin, *Can. J. Chem. Eng.* **2017**, *95*, 2398.
[46] M. Arjmandi, M. Pakizeh, *J. Ind. Eng. Chem.* **2014**, *20*, 3857.
[47] P. Asoka-Kumar, M. Alatalo, A. C. VJ Ghosh, B. Kruseman, K. G. L. Nielsen, *Phys. Rev. Lett.* **1996**, *77*, 2097.
[48] S. Li, X. Jiang, Q. Yang, L. Shao, *Chem. Eng. Res. Des.* **2017**, *122*, 280.
[49] M. Sadeghi, M. A. Semsarzadeh, H. Moadel, *J. Membrane Sci.* **2009**, *331*, 21.
[50] M. Wang, Z. Wang, N. Li, J. Liao, S. Zhao, J. Wang, S. Wang, *J. Membrane Sci.* **2015**, *495*, 252.
[51] N. Konnertz, Y. Ding, W. J. Harrison, P. M. Budd, A. Schönhals, M. Böhning, *J. Membrane Sci.* **2017**, *529*, 274.

How to cite this article: Swapna VP, Kaliyathan AV, Abhisha VS, et al. Changes in free volume and gas permeation properties of poly (vinyl alcohol) nanocomposite membranes modified using cage-structured polyhedral oligomeric silsesquioxane. *J Appl Polym Sci*. 2020; e49953. https://doi.org/10.1002/app.49953